

## Radical Decay and Color Formation at Various Temperatures in Unplasticized Poly(vinyl chloride) Irradiated in Vacuo at 25°C.

G. J. ATCHISON, *Radiochemistry Research Laboratory, The Dow Chemical Company, Midland, Michigan*

### INTRODUCTION

Many investigators have observed the presence of long-lived free radicals (unpaired electrons) in irradiated poly(vinyl chloride)<sup>1,2,4-11</sup> but quantitative measurements of both radical concentration and color have not been reported. The present investigation was carried out to compare absolute radical concentration changes with quantitative changes in absorption in the visible region of the spectrum by the irradiated polymer.

### EXPERIMENTAL

All samples were prepared from an unplasticized poly(vinyl chloride) powder (Dow batch 6054). Moldings were prepared from the powder in a small laboratory press so that part of the finished molding was approximately 0.004 in. thick while the remainder was 0.06 in. thick. The thick sections were used for EPR radical measurements and the thin sections were used for color measurements.

Samples for electron paramagnetic resonance (EPR) and optical measurements were placed in a thin-window irradiation cell and pumped on a vacuum manifold at a pressure of less than  $1 \mu$  for a minimum of 116 hrs. prior to irradiation. At the end of the pumping period the samples were irradiated *in vacuo* with 2 m.e.v. electrons to doses of 5.9-7.3 Mrad at ambient temperature.

Immediately after the irradiation the thin-window cell was transferred to an argon-atmosphere glove box and the samples were transferred to EPR and optical cells. The EPR cell was flame-sealed in the absence of oxygen while the optical cell was sealed with rubber gaskets in the absence of oxygen. The EPR cell was then placed in a temperature-controlled EPR cavity and absorption measurements were made over varying periods of time. Absolute radical concentrations were calculated by continual comparison of the area under the EPR absorption curve with the absorption line of a ruby rod cemented to the back of the cavity.<sup>12</sup> The ruby line was calibrated with known samples of the stable radical diphenylpicryl-

hydrazyl. The EPR values are believed to be correct to  $\pm 15\%$  on the basis of the calibration data. The optical cell was placed in a temperature-controlled cell holder in a recording spectrophotometer, and optical density measurements were recorded simultaneously with the recording of the EPR absorption data.

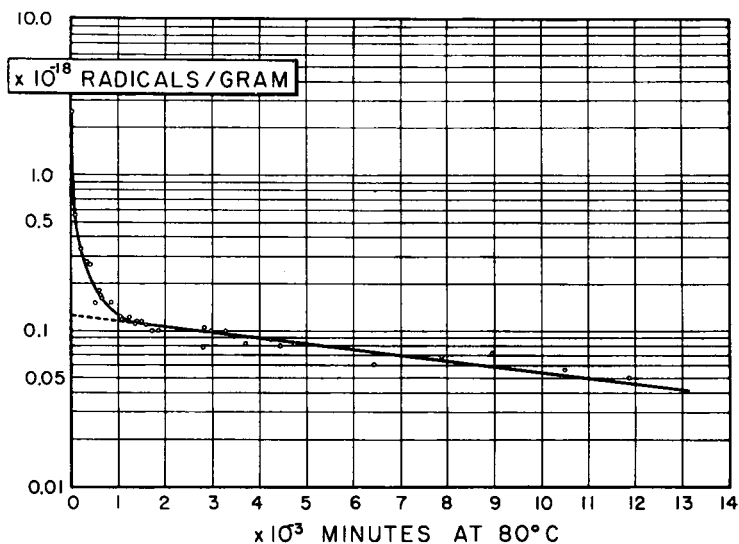


Fig. 1. Concentration of radicals produced at room temperature as a function of storage time at  $80^\circ\text{C}$ .

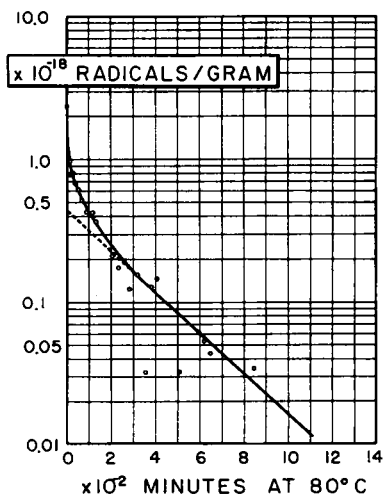


Fig. 2. Concentration of radicals as a function of storage time at  $80^\circ\text{C}$ , after subtracting long-lived component.

## RESULTS

## Radical Concentration and Radical Decay from EPR Data

Measurements of radical concentrations were made at temperatures of 80, 55, and 30°C. Semilogarithmic plots of the absolute concentration against time after the start of heating are given in Figures 1, 4, and 7 for

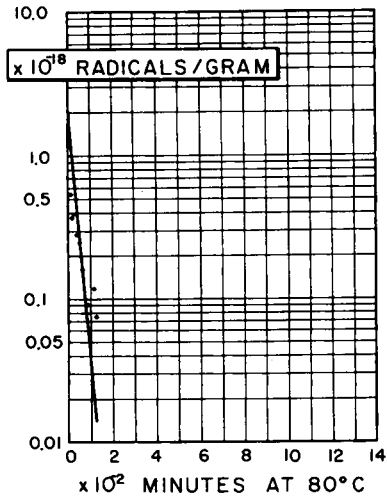


Fig. 3. Concentration of radicals as a function of storage time at 80°C. after subtracting long-lived and intermediate-lived components.

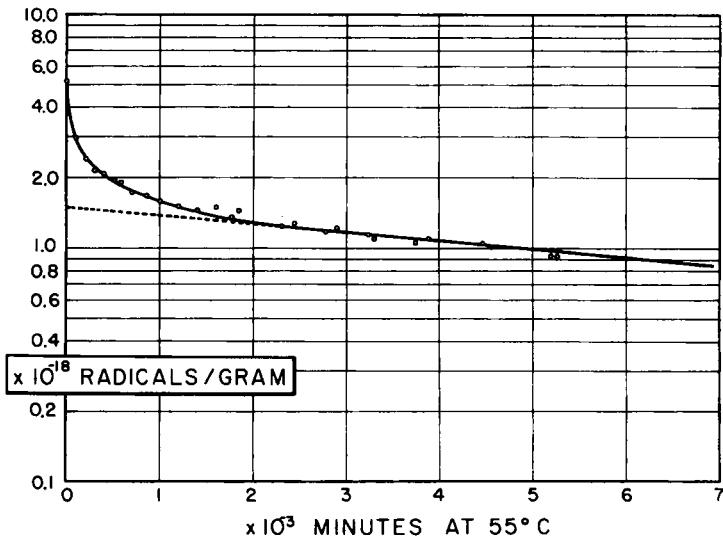


Fig. 4. Concentration of radicals produced at room temperature as a function of storage time at 55°C.

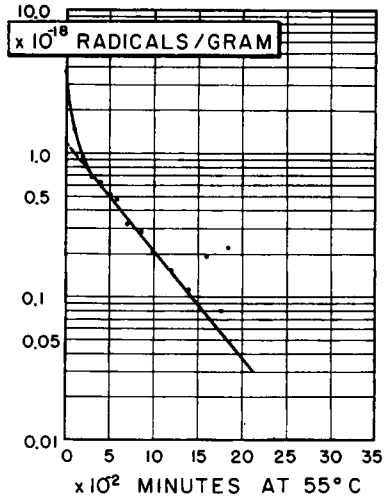


Fig. 5. Concentration of radicals as a function of storage time at 55°C. after subtracting long-lived component.

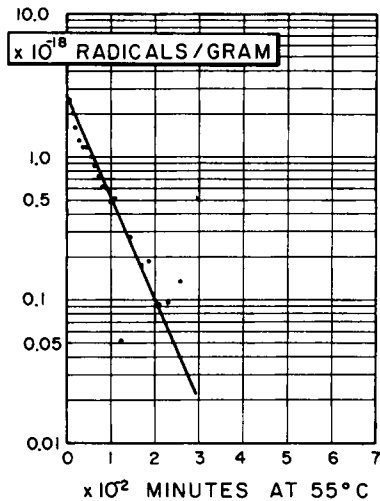


Fig. 6. Concentration of radicals as a function of storage time at 55°C. after subtracting long-lived and intermediate-lived components.

the three samples. Each of these curves was treated as a composite of several exponential decay curves by applying a "peeling-off" analysis. This produced the decay curves for 80°C. shown in Figures 2 and 3, for 55°C. shown in Figures 5 and 6, and for 30°C. shown in Figures 8 and 9. From these plots it is concluded that at each temperature three radical species were present, each decaying independently and with the half-life values given in Table I.

TABLE I  
Half-life Values of Radical Species from Radical Decay Curves

Temperature, °C.	80	55	30
Short-lived radical, min.	20	40	54
Intermediate-lived radical, min.	210	400	720
Long-lived radical, hr.	135	141	3200

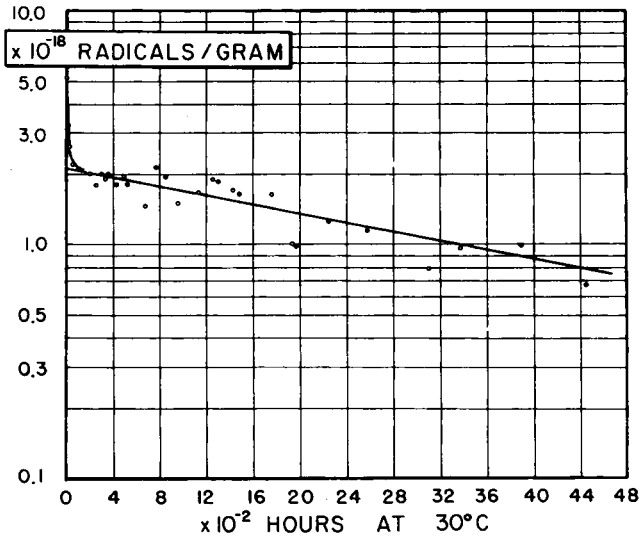


Fig. 7. Concentration of radicals produced at room temperature as a function of storage time at 30°C.

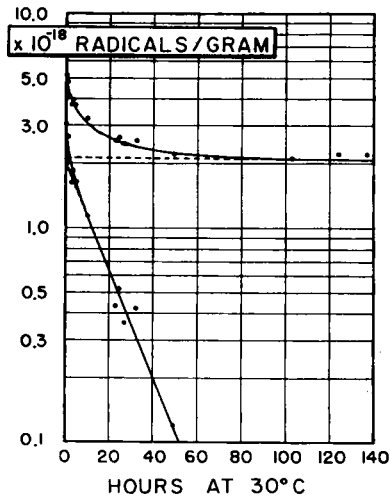


Fig. 8. Concentration of radicals as a function of storage time at 30°C. after subtracting long-lived component. Top curve is a replot of part of Figure 7 on an expanded time scale.

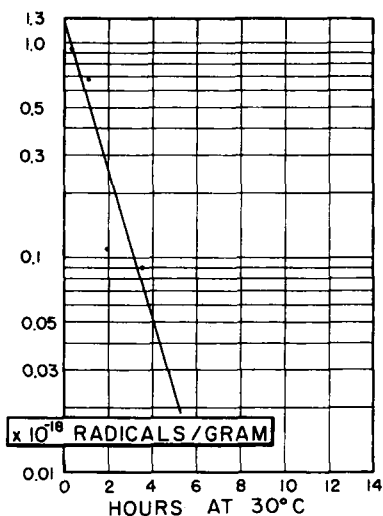


Fig. 9. Concentration of radicals as a function of storage time at 30°C. after subtracting long-lived and intermediate-lived components.

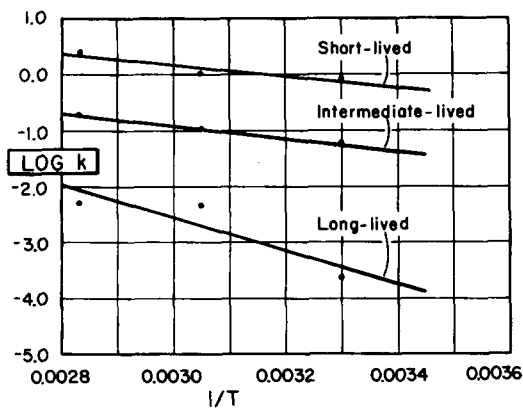


Fig. 10. Log  $k$  vs.  $1/T$  plot for decay of radicals produced at room temperature.

The exponential decay of the radical concentrations indicates that the radicals were decaying by first-order reactions.

### Activation Energy of Radical Decay Reactions

Rate constants for the decay of each radical at the three temperatures were calculated from the radical decay data. An Arrhenius plot was made from these data for each radical species, as shown in Figure 10. Activation energies, calculated from the slopes of these plots, are 4.4, 5.0, and 13.7 kcal./mole for the short-lived, intermediate-lived, and long-lived radicals, respectively.

### G Values of Radical Formation

The radical concentrations observed at the beginning of the heating period were corrected for those short-lived and intermediate-lived radicals which decayed at room temperature during the interval between the end of the irradiation and the beginning of the heating period (37–64 min.). The sums of the concentrations of the three radicals present at the end of the irradiation period were used to calculate  $G$  values of radical formation *in vacuo* at room temperature. The results are given in Table II.

TABLE II  
 $G$  Values of Radical Formation *in Vacuo* at 25°C.

Temp. during EPR	Dose, Mrad.	Time after irradiation, before heating	Tot. radicals/g. at end of irradiation	$G$ (radicals)
30°C.	6.9	60 min.	$6.82 \times 10^{18}$	1.6
55°C.	7.3	64 min.	$9.18 \times 10^{18}$	2.0
80°C.	5.9	37 min.	$5.30 \times 10^{18}$	1.4

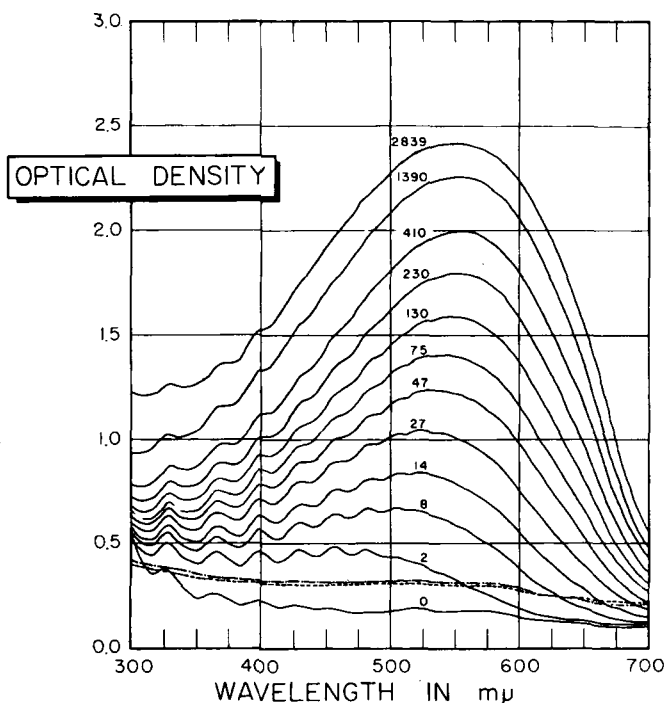


Fig. 11. Development of color during storage at 80°C. after irradiation at room temperature: numbers on curve are minutes at 80°C. (—) sample irradiated at 25°C. and then held at 80°C.; (---) duplicate sample not irradiated and at 25°C.; (-.-) duplicate sample not irradiated but held 180 min. at 80°C.

### Formation of Color in the Irradiated Polymer

The thin sections of the irradiated samples (approximately 0.004 in. thick) mounted in a sealed quartz-window cell were maintained at a constant temperature in a temperature-controlled massive brass cell holder designed to fit the sample compartment of a Cary Model 11 spectrophotometer. The thin sections had had exactly the same thermal history, evacuation, and irradiation as the EPR samples. Optical density curves in the range of 300–700  $m\mu$  were obtained at various times after the beginning of heating, as shown in Figures 11–13. The numbers on each absorption curve are time after the start of heating in minutes for Figures 11 and 12 and in hours for Figure 13.

The fine-structure absorption reported earlier<sup>2</sup> is very pronounced in the spectra of the thin sections, especially at the 30° temperature. Examination of the optical data shows a wide absorption maximum in the region of 500–550  $m\mu$  and a series of seven absorption peaks superimposed upon the

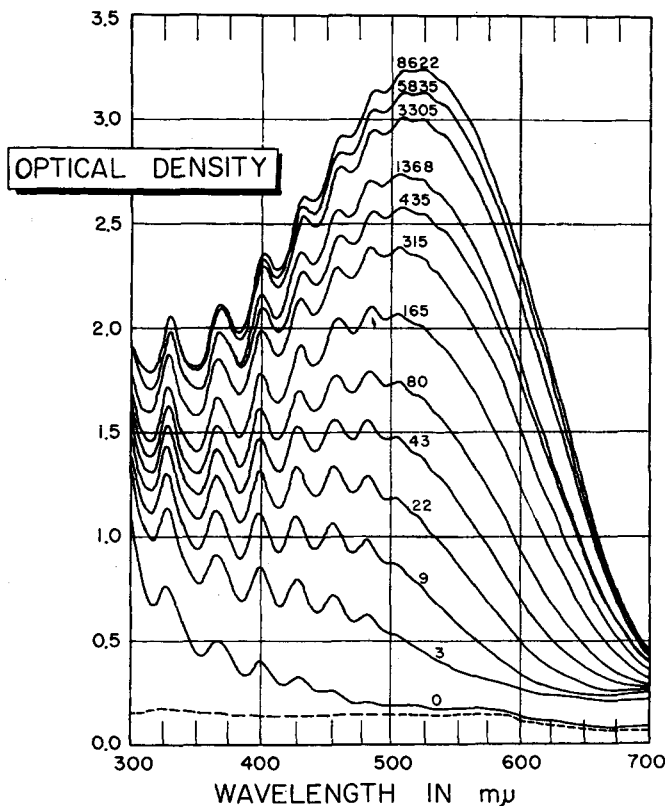


Fig. 12. Development of color during storage at 55°C. after irradiation at room temperature: numbers on curves are minutes at 55°C.; (—) sample irradiated at 25°C. and then held at 55°C.; (---) duplicate sample not irradiated and at 25°C.



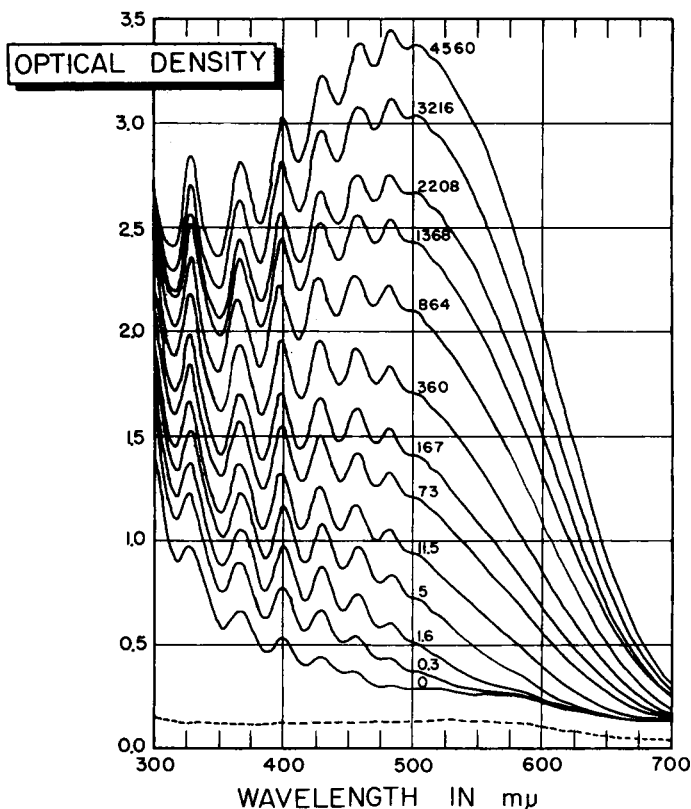


Fig. 13. Development of color during storage at 30°C. after irradiation at room temperature: numbers on curves are hours at 30°C.; (—) sample irradiated at 25°C. and then held at 30°C.; (---) duplicate sample not irradiated and at 25°C.

broad band. The fine-structure peaks show maxima at 505–510, 483–485, 458–460, 430–435, 400–405, 364–365, and 329–330  $m\mu$ . The banded fine-structure peaks tend to broaden at higher temperature, while the broad absorption maximum shifts toward a longer wavelength.

#### Relationship of Color to Radical Concentration

The optical and EPR data obtained at the 30°C. storage temperature were used for the following measurements. The fine structure consists of peaks superimposed on a broad absorption band, as shown in Figure 14, which is a reproduction of part of the data given in Figure 13. Each of the optical density curves of the 30° sample was treated in a similar manner. Relative concentration values were calculated for the material producing each of the absorption peaks and the broad band shown in Figure 13. The optical density at the absorption maximum was measured at the various times and divided by the optical density at zero heating time. These measurements were based on the assumption that the material responsible

for the absorption obeys Beer's law. Thus, a series of relative concentrations with a concentration of unity at zero time was obtained. Radical concentration values corresponding to the time of the taking of the optical

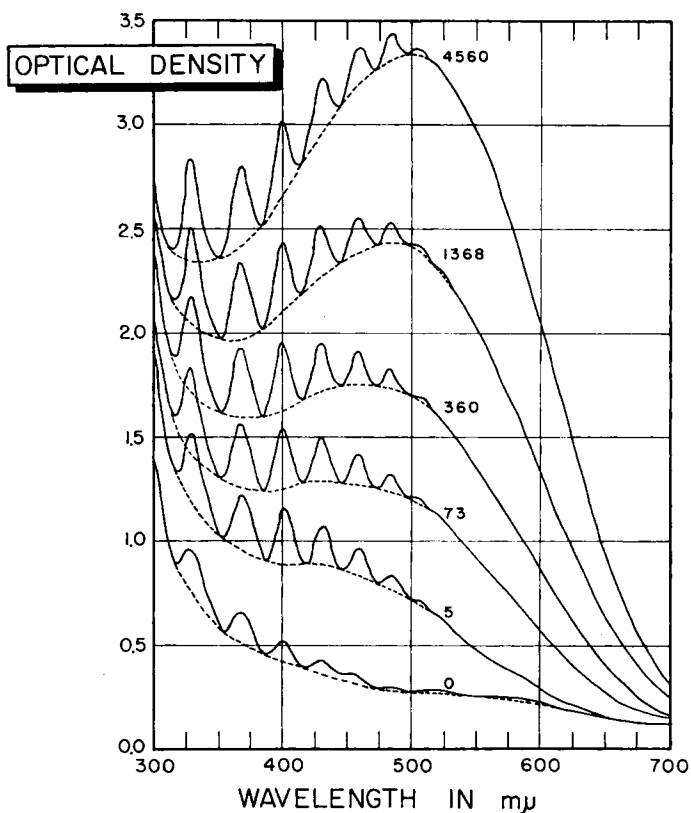


Fig. 14. Replot of part of Figure 13, showing fine-structure peaks superimposed upon broad absorption band.

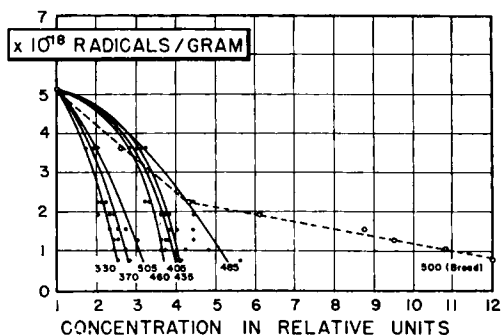


Fig. 15. Concentration of material producing absorption maxima versus total radical concentration during storage at 30°C. Numbers are absorption maxima in millimicrons.

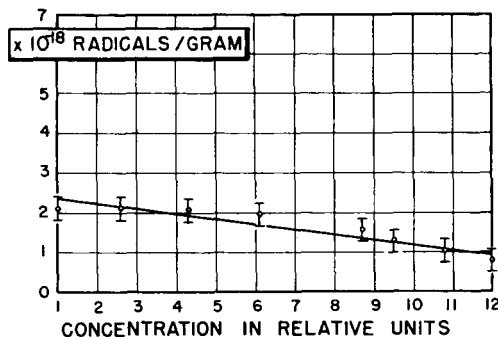


Fig. 16. Concentration of material producing broad absorption band versus concentration of long-lived radicals during storage at 30°C.

data were obtained from the decay curves in Figures 7 and 8. The resulting relationship between relative concentration of absorber and radical content of the sample are plotted in Figure 15. The concentration of the material producing the broad band increases more rapidly than does the concentration of the material causing the fine structure. As the short-lived radicals decay the broad band assumes an almost linear relationship with the decrease in radical concentration. This is shown more clearly in Figure 16, where the relative concentration of the material producing the broad band is plotted against the concentration of the long-lived radical. This shows the concentration of the color-producing material to be inversely proportional to the concentration of the long-lived radical within the uncertainty of the radical concentration measurements. This is in agreement with the qualitative color data of Lawton and Balwit<sup>5</sup> and of Miller.<sup>4</sup>

#### Estimation of Conjugated Double Bond Chain Length

The formation of the yellow to red-black color in irradiated poly(vinyl chloride) has been explained by several investigators as being due to the formation of long sequences of conjugated double bonds.<sup>1-5</sup> The question of the length of the conjugated double bond chain or chains has not been answered. The only clue to the answer so far is the presence of the fine structure in the absorption spectra of the irradiated polymer. The data obtained in this investigation, shown in Figure 13, are the most sharply defined fine structure so far observed. This type of fine structure is characteristic of the absorption spectra of long-chain polyenes. Recent work by Sondheimer et al.<sup>13</sup> on the synthesis of compounds of the type  $H(CH=CH)_nH$  with  $n$  values of 3-10 shows that these compounds obey the Lewis-Calvin relationship<sup>14</sup> ( $\lambda^2 = kn$ ) fairly well. Each of the compounds prepared exhibited four peaks (designated A to D, D being at the longest wavelength). A plot of the  $n$  values against the squares of the wavelengths for each of the four longest wavelength maxima produced straight lines as far as  $n = 7$ , small deviations from straight lines occurring for the higher compounds. The data given by Sondheimer et al. have

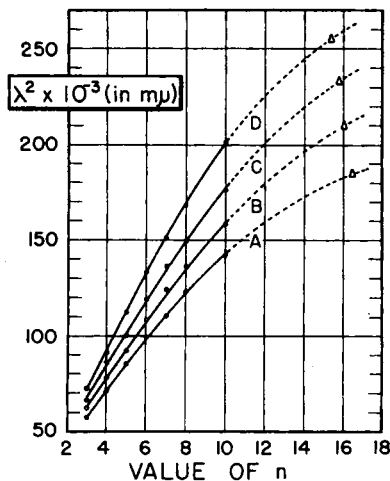


Fig. 17. Relationship between squares of the wavelengths and the values of  $n$  for absorption maxima of conjugated polyenes: (O) data of Sondheimer et al.<sup>13</sup> for  $\text{H}(\text{CH}=\text{CH})_n\text{H}$  in  $\text{Et}_2\text{O}$ ; ( $\Delta$ ) data of this work.

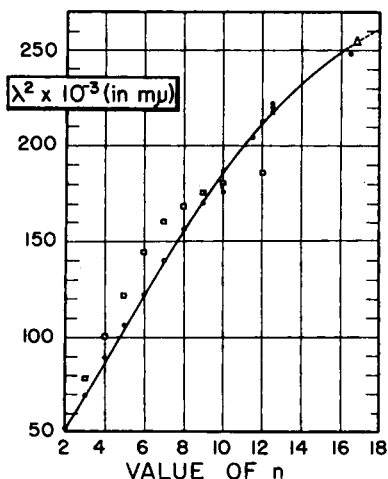


Fig. 18. Relationship between the square of the wavelength of the longest absorption maximum and the value of  $n$  for polyenes: ( $\Delta$ ) data of this work; (O) data of Bohlmann and Mannhardt<sup>14</sup> for  $\text{CH}_3(\text{CH}=\text{CH})_n\text{CH}_3$  in  $\text{Et}_2\text{O}$ ; ( $\square$ ) data of Nayler and Whiting,<sup>15</sup> in  $\text{CHCl}_3$ .

been plotted in Figure 17 and each of the four curves has been extrapolated to higher  $n$  values. The  $\lambda^2$  values of the four longest fine-structure peaks in the irradiated poly(vinyl chloride) spectrum have been plotted on the same coordinates. From the location of these points it is indicated that the observed fine structure is due to a conjugated polyene with an  $n$  value of approximately 16. A similar comparison is made in Figure 18 with data

of Bohlmann and Mannhardt<sup>15</sup> for the wavelength of the longest absorption maxima of compounds of the type  $\text{CH}_3(\text{CH}=\text{CH})_n\text{CH}_3$ . In this case an  $n$  value of approximately 17 is indicated. The data of Nayler and Whiting,<sup>16</sup> however, for the same class of compounds, indicates a leveling-off of the curve at a much lower value of  $n$ .

The polyenes synthesized by Sondheimer et al. each had only four definite absorption peaks, but there are indications in their optical data for polyenes of  $n = 6, 8,$  and  $10$  that the number of peaks may increase as the value of  $n$  increases. This assumption was made in the above comparison and only the four peaks of longest wavelength (out of the seven observed in the visible region in the irradiated polymer) were compared with the published data. In addition, the optical data from the above publications were obtained in solution while the data of this investigation were obtained from solid samples, so an exact comparison cannot be made. The comparison does, however, indicate the presence of a conjugated double bond compound of  $n = 16-17$ .

The explanation of the cause of the broad absorption band (which was found to vary inversely with the concentration of the long-lived radical species) still remains to be given. It may be that the broad band is due to the presence of a number of polyenes with such a distribution of  $n$  values as to produce an absorption envelope of broad shape. If this is correct, then some mechanism must be in operation which produces a selective and rather stable concentration of  $n = 16-17$  polyenes in addition to a wide distribution of  $n$  values.

## CONCLUSIONS

The radicals, which are produced in unplasticized poly(vinyl chloride) by high-energy irradiation at room temperature in the absence of air, will decay over long periods of time with temperature-dependent rates. The color of the irradiated polymer increases as the radicals decay. Optical data in the visible region show a broad absorption band at approximately  $500 \text{ m}\mu$  with a series of seven sharp peaks superimposed upon the broad absorption. The sharp peaks are consistent with literature data for a polyene chain of  $16-17$  conjugated double bonds. The broad band, which is inversely proportional to the long-lived radical concentration, may be due to an absorption envelope produced by polyenes of a distribution of  $n$  values.

The author wishes to thank B. Loy for the EPR measurements.

## References

1. Chapiro, A., *J. Chim. Phys.*, **53**, 895 (1956).
2. Atchison, G. J., *J. Polymer Sci.*, **49**, 385 (1961).
3. Winkler, D. E., *J. Polymer Sci.*, **35**, 3 (1959).
4. Miller, A. A., *J. Phys. Chem.*, **63**, 1755 (1959).

5. Lawton, E. J., and J. S. Balwit, *J. Phys. Chem.*, **65**, 815 (1961).
6. Kuri, Z., H. Ueda, and S. Shida, *J. Chem. Phys.*, **32**, 371 (1960).
7. Abraham, R. J., and D. H. Whiffen, *Trans. Faraday Soc.*, **54**, 1291 (1958).
8. Ueda, H., Z. Kuri, and S. Shida, *J. Appl. Polymer Sci.*, **5**, 478 (1961).
9. Kuri, Z., and H. Ueda, *J. Polymer Sci.*, **50**, 349 (1961).
10. Loy, B. R., *J. Polymer Sci.*, **50**, 245 (1961).
11. Ohnishi, S., Y. Ikeda, S. Sugimoto, and I. Netta, *J. Polymer Sci.*, **47**, 503 (1960).
12. Singer, L. S., *J. Appl. Phys.*, **30**, 1463 (1959).
13. Sondheimer, F., D. Ben-Efraim, and R. Wolovsky, *J. Am. Chem. Soc.*, **83**, 1675 (1961).
14. Lewis, G. N., and M. Calvin, *Chem. Revs.*, **25**, 273 (1939).
15. Bohlmann, F., and H. Mannhardt, *Chem. Ber.*, **89**, 1307 (1956).
16. Naylor, P., and M. C. Whiting, *J. Chem. Soc. (London)*, **1955**, 3037.

### Synopsis

Moldings were irradiated at ambient temperature *in vacuo* with 2 m.e.v. electrons to doses of 5.9–7.3 Mrad. The decay of radicals was followed by EPR spectroscopy at 80, 55, and 30°C. while simultaneous extinction measurements were made at 300–700  $m\mu$  with a recording spectrophotometer. The radical decay data indicated the presence of three species at each temperature, decaying exponentially with time, with half-lives of 20 min., 210 min., and 135 hrs. at 80°C. of 40 min., 400 min., and 141 hrs. at 55°C., and of 54 min., 720 min., and 3200 hrs. at 30°C. *G* values of 1.6, 2.0, and 1.4 were obtained for radical formation at 25°C. by back-extrapolation of decay curves from the three temperatures to the end of the irradiation period. The activation energy of radical decay was found to be 4.4, 5.0, and 13.7 kcal./mole for the short-lived, intermediate-lived, and long-lived radicals, respectively. The optical data has a broad absorption maximum at 500–550  $m\mu$  and a series of seven absorption peaks with maxima at 505–510, 483–485, 458–460, 430–435, 400–405, 364–365, and 329–330  $m\mu$ . The concentration of the material producing the broad bands was found to be inversely proportional to the long-lived radical concentration. The fine-structure peaks are consistent with literature data for a polyene chain of 16–17 conjugated double bonds.

### Résumé

Des échantillons fondus ont été irradiés à température ambiante sous vide avec des électrons de 2 Mev à des doses de 5.9–7.3 mégarads. La diminution de radicaux a été suivie par spectroscopie EPR à 80°, 55° et 30°C et des mesures d'extinction ont été effectuées simultanément de 300 à 700  $m\mu$  au moyen d'un spectrophotomètre enregistreur. Les résultats sur la disparition progressive des radicaux montrent la présence de trois espèces à chaque température. La diminution de concentration se fait exponentiellement avec des durées de demi-vie de 20 min., 210 min. et 135 heures à 80°C; 40 min., 400 min. et 141 heures à 55°C; et 54 min., 720 min. et 3200 heures à 30°C. Les valeurs de *G* de 1.6, 2.0 et 1.4 ont été obtenues pour la formation du radical à 25°C par extrapolation des courbes de décroissance obtenues à trois températures et à la fin de la période d'irradiation. Les énergies d'activation pour la disparition du radical sont de 4.4, 5.0 et 13.7 kcal/mole pour les radicaux de courte durée de vie, de durée de vie moyenne et de longue durée de vie respectivement. Les résultats optiques montrent un large maximum d'absorption à 500–550  $m\mu$  et une série de sept pics d'absorption avec des maxima situés à 505–510, 483–485, 458–460, 430–435, 400–405, 364–365 et 329–330  $m\mu$ . On a trouvé que la concentration du produit qui donne une large bande est inversement proportionnelle à la concentration en radicaux de longue durée de vie. Les pics à structure fine sont en accord avec les données de la littérature pour une chaîne polyénique possédant 16–17 doubles liaisons conjuguées.

### Zusammenfassung

Proben wurden bei Raumtemperatur im Vakuum mit 2 MEV-Elektronen bis zu Dosen von 5,9 bis 7,3 megarad bestrahlt. Das Verschwinden der Radikale wurde E.P.R.-spektroskopisch bei 80°, 55° und 30° verfolgt und gleichzeitig Extinktionsmessungen von 300–700 m $\mu$  mit einem automatischen Spektralphotometer durchgeführt. Die Daten für den Radikalabfall liessen die Gegenwart von drei verschiedenen Arten bei jeder Temperatur erkennen, die mit der Zeit exponentiell abklingen und zwar bei 80°C mit Halbwertszeiten von 20 min, 210 min und 135 h; bei 55° mit 40 min, 400 min und 141 h und bei 30° mit 54 min, 720 min und 3200 h. Durch Rückextrapolation der Abklingkurven bei den drei Temperaturen auf das Ende der Bestrahlungsperiode wurden *G*-Werte für die Radikalbildung von 1,6, 2,0 und 1,4 erhalten. Die Aktivierungsenergie des Abklingens der Radikale ergab sich zu 4,4, 5,0 und 13,7 kcal/Mol für die kurzlebigen, bzw. mittleren bzw. langlebigen Radikale. Die optischen Daten zeigten ein breites Absorptionsmaximum bei 500–550 m $\mu$  und eine Reihe von 7 Absorptionsspitzen mit Maxima bei 505–510, 483–485, 458–460, 430–435, 400–405, 364–365 und 329–330 m $\mu$ . Die Konzentration der für die breite Bande verantwortlichen Substanz erwies sich als umgekehrt proportional zur Konzentration der langlebigen Radikale. Die Feinstrukturmaxima stimmen mit Literatursaten für eine Polyenkette von 16–17 konjugierten Doppelbindungen überein.

Received May 14, 1962